Coalescence of fullerene cages: Topology, energetics, and molecular dynamics simulation

Yufeng Zhao, Richard E. Smalley, and Boris I. Yakobson*
Center for Nanoscale Science and Technology and Department of Mechanical Engineering and Materials Science, Rice University, Houston, Texas 77005

(Received 21 June 2002; published 18 November 2002)

Sequential atomic rearrangements leading to the coalescence of fullerene cages or tubes are derived by topological analysis. Qualitative reasoning assists the search for the minimum-energy path, which consists of a jump-to-contact formation of covalent bonds between the separate cages and the following ''plastic flow'' by exclusively Stone-Wales bond rotations. A connecting neck forms and grows gradually until the separate clusters are completely fused into a coherent unit. The most favorable path is determined by comparison of the calculated energies and is further supported by molecular dynamics simulations. Results are presented for $C_{60}+C_{60}$, C_{60}+tube, cap-to-cap, cap-to-wall, and wall-to-wall coalescence of nanotubes of different types.

DOI: 10.1103/PhysRevB.66.195409 PACS number(s): 61.46.+w, 81.07.−b

I. INTRODUCTION

Joining nanoscale units in singular elements is interesting from practical (for nano- and molecular electronics and mechanics) as well as fundamental (possible atomic mechanism) points of view. Examples of small fullerene fusion have been reported[1–5] and the lateral merging (diameter doubling) of carbon nanotubes (CNT's) has been observed and simulated.[6,7] In contrast, head-to-head CNT coalescence remains unexplored. If feasible, such ''welding'' could increase the connectivity in CNT arrays (bundles and ropes) and crystals, and improve the mechanical, thermal, and electrical material properties. Determining the paths of tube coalescence can shed light on the underlying mechanism of recently reported condensed phase conversion[8] and CNT crystal synthesis[9] from C_{60} components.

In our recent work,[10] a possibility of such coalescence has been demonstrated and a few examples presented. This article provides a more systematic description of the method of path identification and addresses several other cases of coalescence. We present a few empirical rules that can assist in analysis of any other particular combination of merging units. The content of this article is organized as follows. In Sec. II, some general considerations for the topological construction of reaction paths are described. In Sec. III, explicit topological transformation sequences for several archetypal tube types are derived. Energies of the series of intermediate configurations are computed, in order to evaluate the physical accessibility of the final minimum-energy state. Molecular dynamics (MD) simulation results are presented in Sec. IV to show the role of configuration entropy at high temperatures.

II. BASIC CONSIDERATION

In this section, we first discuss the feasibility of perfect cap-to-cap coalescence of fullerenes or nanotubes—that is, two cages or end-to-end oriented tubes merging into a perfect unit. A few guiding principles are drawn from the viewpoint of seeking the minimum-energy path. Detailed constraint rules are derived from these guiding principles and the structural features of the capped tube.

A. Preliminary considerations and projection

The geometrical surface area of a sphere equals exactly that of a cylinder of the same diameter and length. Physically, the strain energy of a spherical shell is higher than that of a tube, and the reduction of energy can provide a driving force for transformation.

To justify the topological feasibility of coalescence, we have to examine the atomic structure of a capped tube. Only the icosahedral caps are discussed here for two reasons: the icosahedral cap is the most stable according to the ''isolated pentagon role,'' [11] and the icosahedral cap can be considered as a perfect cap: that is, its shape is the closest to a perfect semisphere. Using the projection method,[12] a CNT can be flattened into a graphite sheet and its icosahedral cap into five equilateral triangles. Actually, a tube can be cut into two tubes with caps following Fig. 1(a), which shows a projection map of a (10,10) tube. The circumferential zigzag line along which the tube is cut forms five triangles attached to each side. By wrapping up each flat sheet into a cylinder and folding up the triangles so that their top vertices all meet [Fig. 1(b)], a tube with icosahedral caps will be formed. But this cutting involves a high energy of breaking bonds and is physically unfeasible.

In this study, we illustrate the cap structures in a geodesic projection, where the five equilateral triangles are stretched to fill the same circumferential length as that of the tube [Fig. 1(c)] and the top straight line with five sections is the projected apex pentagon. This way the cap is stretched and flattened in the projection map, but the exact connectivity of the bonds of the three-dimensional (3D) structures is preserved.

B. General guidelines

Physically, the coalescence will more likely proceed along some minimum-energy path which is very difficult to determine for a process with many degrees of freedom, but several qualitative guidelines can be drawn.

(a) Only lower-energy gradual structural transformations are of interest (not high-energy fragmentation and rebuilding as in graphite ablation for fullerene synthesis or ''cutting'' as in the above illustration). A plausible continuous scenario involves an emerging and widening neck,

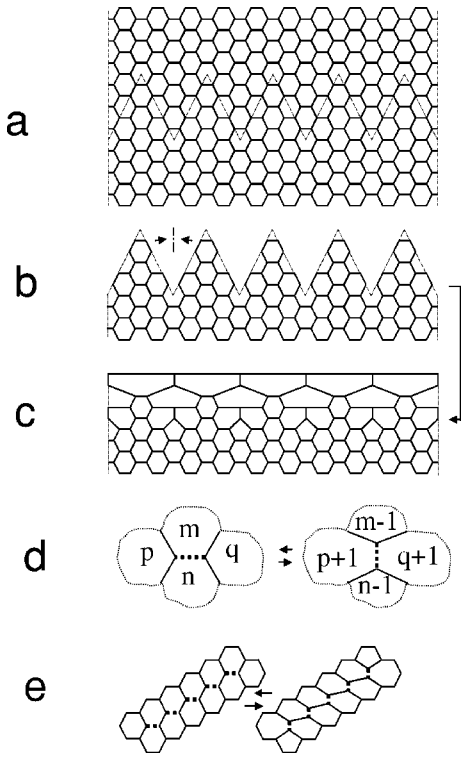

FIG. 1. Projection map and SW rotation: (a) a section of projected (10,10) tube with open ends (top and bottom), (b) a half of the tube cut along the zigzag line in (a), (c) a geodesic projection of the capped (10,10) tube, (d) Stone-Wales transformation, and (e) successive SW rotations of parallel bonds in a zigzag path. In all the figures of this paper, solid lines are normal bonds, the bonds subject to SW flips are dotted thicker lines, dashed lines are bonds broken or to be generated, and very thin dot-dashed lines are the cutting trace for projection.

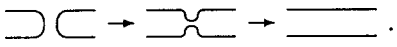

Here, a tiny, primary neck (a short section of a tube) is first formed between the caps and then widens by dissolving the caps, until it attains the diameter of the original pieces and a single tube is formed. So the emerging of the primary neck and its further growth can be distinguished.

(b) Such gradual ''morphing'' must be achieved through atomic steps of low energy, avoiding wherever possible dangling bonds, vacancies, or interstitials. Studies of fullerene isomerization[13–16] and mechanical relaxation in nanotubes[17] indicate that the lowest barrier step is a single bond flip rotation of ''pyracylene'' or Stone-Wales (SW) type.[16,18] This leads to an even more taxing question: can the fusion occur exclusively by a sequence of SW steps? The answer is yes, as described below.

(c) We seek the lowest-energy path among the SW routes and must avoid highly distorted polygons below pentagons or above heptagons and keep the number of these low.

(d) More symmetric structures should be preferred at every step to avoid high deformation. At a high temperature, of course, entropy plays an important role and actual intermediate configurations can significantly deviate from those theoretically proposed below. Indeed, MD simulations show noticeably higher energies (Fig. 3 in Ref. 10).

In the above process, we assume that the 2D shell morphology is properly preserved, which is not just a topological limitation for high-quality coalescence. More significantly, the 2D shell (sp^2) is more compliant than 3D (sp^3) bulk[19] and can tolerate much more distortion,[20] which reduces energy of the intermediate structures with low symmetry. We found that even a few sp^3 atoms introduced in the earlier intermediate stage can greatly increase the barrier.

C. Specific constraint rules

To facilitate the search of the actual fusion path, more detailed rules have been drawn. In addition to the above guiding principles, they take into consideration the structural features of the caps and the properties of SW rotation.

In Fig. 1(a), notice that the triangles in the two sides of the cutting line can be fitted to a perfect tube in a complementary way. This requires the two caps to face in a staggered fashion, with the apex pentagons misoriented by $\pi/5$. Due to the fivefold symmetry, the structure can be divided into five identical units circumferentially. We will take the advantage of these two features to prescribe the rules.

A SW operation can be presented by a diagram as in Fig. 1(d). In a 2D sp^2 lattice, each bond (dashed line) is surrounded by four nearest polygons. After rotation of the bond, the edge number of two of the polygons will decrease by 1 and that of the other two increases. It is easy to deduce that successive rotations of the parallel bonds in a zigzag path [Fig. 1(e)] only change the number of edges of polygons at the ends of the path. This observation helps to lower the number of nonhexagons in derivation of the coalescence sequence.

Below we give several assisting rules.

(a) The initial arrangement of the two caps to be coalesced should be staggered. This is reflected in the geodesic projection map as the displacement of nodes of the apex pentagons [Fig. 2(a)].

(b) The SW operations should proceed through circumferential cycles. After the primary neck (with fivefold symmetry) is formed, each cycle should be divided into five identical subsequences.

(c) In each cycle, the first choice subsequence should be a zigzag path [see Fig. 1(e)] which terminates at some defects (nonhexagon) and might turn them into hexagons after rotations.

(d) Shorter subsequences are preferred to avoid significant asymmetry.

(e) The bonds to be rotated should be in or near the axial direction so that their rotations lead to mass transport outward from the axis, therefore widening the neck.

(f) After a full circumferential cycle of SW rotations, the number of nonhexagons should not increase.

These rules assist in derivation of the SW sequences for coalescence. The complex transformation process can be reduced to a few optional sequences, among which the most favorable path can be determined by energy calculations.

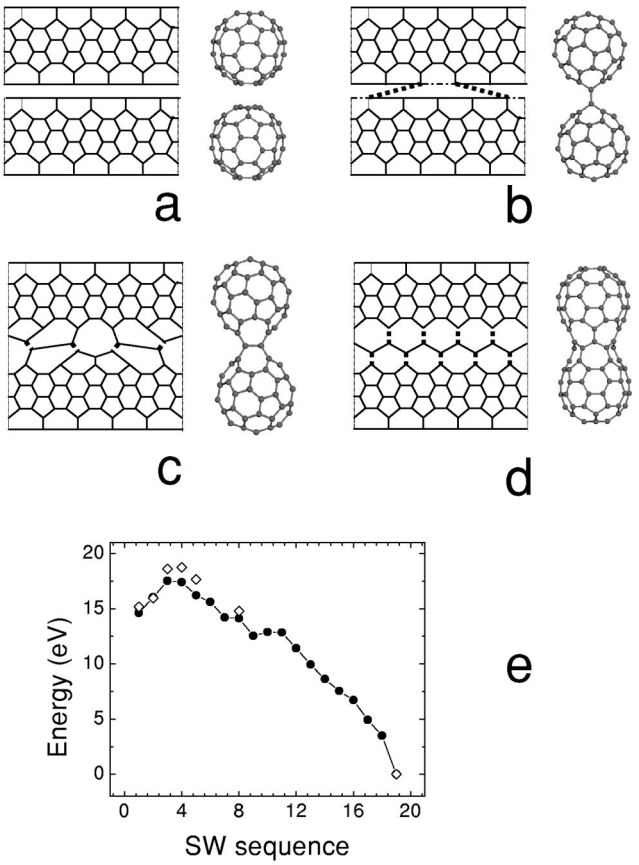

FIG. 2. Geodesic projection and 3D models show the transformations from a pair of separate fullerenes (a) to a short section of a capped (5,5) tube. Primary ''polymerization'' links form [(b), dotted lines] as two other bonds break [(b), dashed lines]. The $\pi/2$ rotations of the links and the SW flips of the four other bonds in (c) produce a (5,0) neck (d). It widens by means of another ten SW rotations, forming a section of a capped (5,5) tubule (not shown). The corresponding energy curve is shown in (e), where the solid circles are the tight-binding result, and the open diamond points are density functional theory results.

III. DYNAMIC TOPOLOGY AND ENERGETICS

In this section, we present transformation sequences for the coalescence of several archetypal cages and calculate the intermediate energies. The projection method[12] is employed for the 2D design of the structural sequences. Their 3D ball-stick model is implemented using visual molecular dynamics (VMD).[21] Coordinates of all the intermediate structures are also generated using VMD and then optimized using an empirical interatomic potential.[22] More accurate energy calculations are performed on the basis of the tight-binding method[23] and some are verified with density functional *ab initio* methods.[24] In actual calculations, the tubes are cut long enough to remove the interaction between the open ends and the cap or junction; all the open ends are saturated with hydrogen atoms.

A. Primary neck formation and fusion of fullerenes

To identify the primary neck and its formation steps, we notice that the two staggered apex pentagons [Fig. 2(a)] form the same atomic configuration as the two rows of a (5,0) tube, except that the diameter and bonding are different. Consequently, a (5,0) primary neck can be formed from the two pentagons facing each other. This process is the same for the coalescence of various tubes, but here we consider it for the smallest system of a properly oriented C_{60} pair. Obviously, the initial transition from the disconnected manifolds to a single continuous network requires out-of-plane atomic excursions and the formation of new bonds (cap bonding) is inevitable. That means that sp^3 hybridization must be introduced in the very initial steps. It has been found that a single extra bond cannot stabilize two fullerenes (C_{60}) linked together, while a pair of bonds is sufficient.[25] The sp^3 component is expected to be removed instantly in the next step by breaking two of the original bonds. Therefore two newly formed bonds should be close to each other in order to form a four-member ring with two original bonds in the caps, just as in C_{60} polymerization.[26] The configuration that not only fulfills this condition but also has the best symmetry is shown in Fig. 2(b), where the dotted lines are two new bonds. Once the two old bonds (dashed lines) in the four-member ring break, the unified sp^2 network will be recovered. The next two identical steps are already SW flips rotating the link bonds from the axial (vertical) to the circumferential (horizontal) direction, Figs. 2(b) and 2(c). The caps become connected by two *H*-shaped bridges, with the heptagons at the top and bottom and larger polygonal holes on the sides, Fig. 2(c). Further, four identical SW flips [bonds marked in Fig. 2(c)] follow in a zigzag order along the circumference, eliminating the larger polygons and producing a more regular all-heptagon belt, Fig. 2(d). One can recognize a very short (5,0) neck connecting the initial fullerenes. This way the primary neck is formed through SW rotations following only the initial rebonding step.

Note that ten heptagons appear on both sides of the primary neck. The heptagons are a requirement of the concave (negative curvature[27]) surface near the neck. These ten heptagons can move but will not disappear until the final unit [C_{120} or a short section of capped (5,5) tube] is formed. This is achieved by rotations of the bonds marked in Fig. 2(d).

Generally two C_{60}'s might coalesce from different orientations. However, we found that the final product of the fusion from other orientations (e.g., hexagon to hexagon) is always cages with negative curvature, like the structures found by Strout *et al.*[28] We found that a complete restructuring of the two end caps is required to remove the negative curvature. But these paths always have a much higher barrier because of the unavoidable occurrence of pentagon pairs (a violation of the ''isolated pentagon rule'' [11]).

Experimental coalescence of C_{60}'s inside a CNT has been reported[2,4] at around $T=1500$ K within $t\sim 24$ h. The barrier can be very roughly estimated as $B=4.0-4.5$ eV following

$$B = kT\ln(\nu t), \tag{1}$$

where $\nu\sim 10^{13}$ is the attempt frequency and k is the Boltzman constant.

The above barrier is higher than that (3.8 eV) shown in Fig. 2(e). The difference (0.5–1.0 eV) might be the activa-

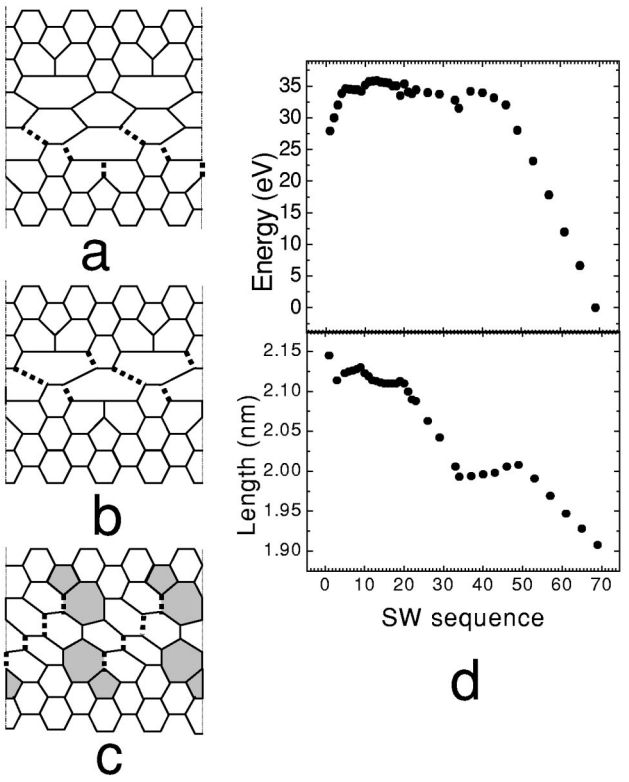

FIG. 3. Projection presentation of coalescence of two (10,10) CNT's: in a sequence similar to Fig. 2, separate caps (not shown) develop a (5,5) neck (a). It shortens (b) and then widens into a (10,5) neck (c). The glide of the shaded 5/7 dislocations completes the annealing into a perfect (10,10) CNT (not shown). Due to the fivefold symmetry, only two cells are displayed. The energy and length evolution in this path are shown in (d).

tion energy of the SW flip taking place at the highest curve point which corresponds to the structure shown in Fig. 2(b). Although the SW barrier for graphite and fullerenes is calculated to be 6–7 eV,[29,30,14] it can be significantly reduced under strain, to 3 eV or lower.[31] The activation energy can also be greatly reduced in a defective local environment.[14] The above two bonds (after breaking the dashed bonds) are much easier to be rotated because the two parts linked by the bonds have no other connections. Furthermore, the collisions with other fullerenes confined in the 1D CNT (Ref. 2) at high temperature exert a compression on the two bonds and will naturally cause the flips in perpendicular direction as shown in Fig. 2(c).

B. Armchair tubes

Obviously, the above SW sequence applies exactly to the coalescence of two (5,5) tubes. We now turn to the case of more common (10,10) CNT's, Fig. 3. Initial cap bonding, the formation of the smallest (5,0) neck, and its widening into a (5,5) neck [Fig. 3(b)] can also follow the path described above for the $C_{60}+C_{60}$ and (5,5)+(5,5) cases. From this point, further SW subsequences shown in Fig. 3 lead to the final perfect (10,10) tube. Cycles of SW flips of the marked bonds in circumferential order gradually widen the neck to the final (10,10) size. Neck formation and growth is general in macroscopic sintering, but the diameter of the nanoscale junction is quantized as it undergoes the transformations (5,0)→(5,5)→(10,5)→(10,10), a perfect cylinder. Remarkably, at the late stage in Fig. 3(c) the distinct 5/7 edge dislocation cores can be recognized. As relaxation continues, these dislocation pairs glide to meet and annihilate, 5/7 +7/5→5/7/7/5→0, all via SW flips only. This completes the coalescence in the theoretical construction, as is also observed in our hands-off MD simulation, and is exactly the reverse of the emergence, split, and glide apart of the 5/7 pairs in relaxation under high tension.[17] Elimination of the last series of 5/7 defects corresponds to the annealing of tilt boundaries between the lattice grains of different orientations, i.e., different chirality: (10,10) next to (10,5) next to another (10,10), Fig. 3(c). The full sequence is animated in 3D models.[32]

Figure 3(d) shows the results (energy and length) of full relaxation for each of the isomers, numbered from the initial separate cages configurations along the paths (essentially the number of SW steps). The length is defined as the distance between the gravity center of the two open ends. Because the length decreases monotonously, a compression force can reduce the barrier and accelerate the coalescence significantly.

Overall the energy change resembles nucleation in a phase transition, with a barrier of 7.8 eV followed by reduction of 35 eV in energy upon completion. Linear slopes at the late stage of coalescence correspond to dislocation pairs gliding down the attraction potential[33] followed by annihilation.

C. Zigzag tubes

The zigzag (15,0) tube has a diameter similar to (10,10). The SW coalescence sequence is shown in Figs. 4(a)–4(d) and Ref. 32. The neck grows following (5,0)→(5,5) →(10,0)→(10,5)→(10,10) stages. Actually, a path almost identical to this is also possible for the coalescence of (10,10) tubes, but the corresponding energy barrier is much higher than the one shown in Fig. 3.

The corresponding energy and length curves are plotted in Fig. 4(e). Notice that the shape of the energy curve is similar with that of the (10,10)+(10,10) case. Even the barrier and energy reduction (7.9 and 33.3 eV) are almost the same. This barrier is much higher than the (5,5)+(5,5) case, which is 3.7 eV. Basically, the barrier increases as the diameter of the tubes and therefore the curvature of the concave area increases.

D. C_{60} with (10,10) tube

Another potentially important[8,9] case involves merging a C_{60} cage to the (10,10) tube. A sequence of projection maps is shown in Fig. 5. Again, there exists a SW path of 63 steps that can be divided into two stages.[32] First, the cap bonding followed by the (5,5) collar formation in Fig. 5(b) can go on exactly as in the (5,5)+(5,5) fusion. Further bond flips are shown in Figs. 5(b) and 5(c). In this process, after the two cycles of SW subsequences as shown in Fig. 5(b), the (5,5)−(10,10) interface will drift towards the (5,5) cap. The SW sequence marked in Fig. 5(c) leads to a complete C_{60}

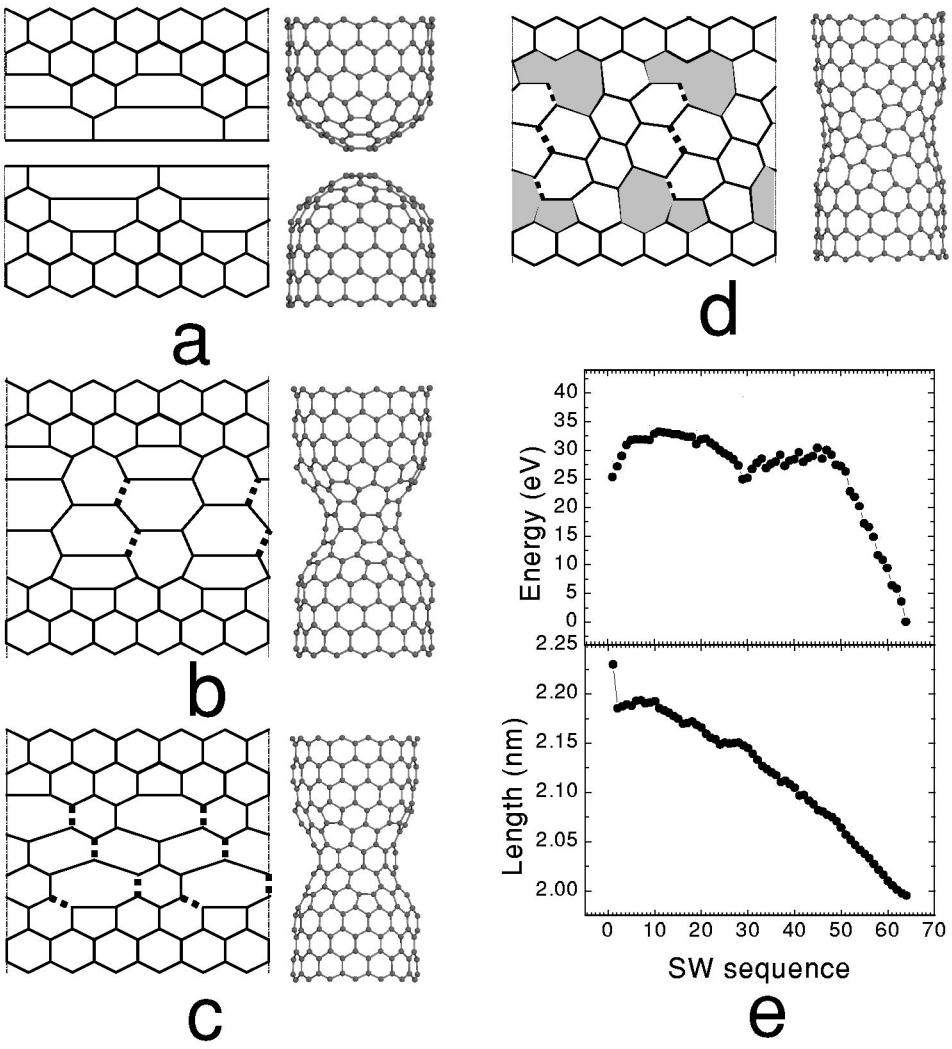

FIG. 4. SW sequence (a)–(d) and energy path (e) for the coalescence of capped (15,0) tubes. This path is similar to that shown in Fig. 3, except that a (10,0) neck appears in (c).

dissolution in the CNT, which thus accrues new material and increases in length by one and half lattice parameters (0.367 nm). Notably, the structure of the cap is completely restored,[32] and the process can recur as the next C_{60} arrives, $C_n + C_{60} \rightarrow C_{n+60}$, etc. From the energy path [Fig. 5(d)], one finds that the energy decreases monotonously after formation of the (5,5) collar. This also means that a (5,5) tube attached to a (10,10) tube can be ''swallowed'' by the latter if the temperature is high enough to overcome the SW barrier.

E. Wall-to-wall coalescence

Diameter doubling of single-walled carbon nanotubes has been observed experimentally.[7] The dynamic process of this wall-to-wall coalescence has been investigated under a transmission electron microscope[6] and with molecular dynamics simulations.[6,34] Although the exact reaction path or atomic rearrangement sequence is ambiguous, a pathway can be suggested for the armchair tube: each pair of atoms linked by a bond (perpendicular to the axis) first rebonds with its counterpair of atoms in the other tube to form a four-member ring. Then the original bonds in the ring break, driven by the curvature. The two tubes will merge into a wider one after all the original bonds in the rings break along the axis (zipping[6]). For the zigzag tube, SW flips are needed to make the horizontal bonds (parallel to the axis) become vertical (perpendicular to axis); the following two steps are exactly the same as in the armchair case. Finally, SW rotations will heal the defects to recover a perfect zigzag lattice.

We present here a purely SW sequence leading to diameter doubling. The supposed initial merging state[6] is shown in Fig. 6(a): two parallel (5,5) tubes have been partially merged into a section of (10,10), while a 12-member, ring serves as a ''vault'' between the (10,10) and the (5,5) domains. Qualitatively, two subsequences of SW rotations make the vault propagate along the axial direction [arrow in Fig. 6(a)]: first, the six bonds belonging to the vault hole in the (10,10) side rotate to reduce the hole into a hexagon and shift it downward; second, rotation of the six bonds leading to vertices of the hole from the (5,5) side again widen it into a 12-member ring. Each cycle shifts the vault a step (2.45 Å)

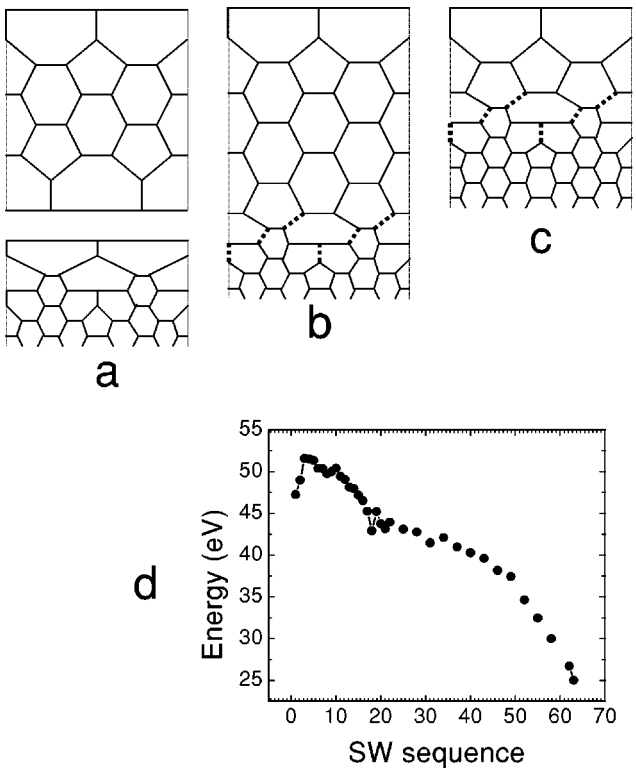

FIG. 5. C_{60} and a (10,10) tube (a) can fuse by first building a (5,5) junction (b) through the same steps as shown in Fig. 2. SW flips of the bonds indicated in (b) shorten the neck, and after two such rounds it transforms into (c). Continuing SW steps in (c) completely dissolve the C_{60} bulge forming a longer (10,10) tubule with the restored perfect cap that permits further fusion processes. The energy curve (d) indicates a lower barrier than that of the (10,10) + (10,10) case.

forward. Successive cycles will merge the two (5,5) tubes into a (10,10) tube following a zipping mechanism. Of course only 12 SW flips cannot accomplish a cycle, because the defects (pentagons, heptagons, and octagons) created by SW rotations must be healed by extra SW rotations. We present here a sequence of 22 SW rotations in which only the nearest and the second-nearest neighbors (polygons) to the vault are involved. Figure 6(c) is the energy curve (empirical potential[22]) covering three successive zipping cycles. As could be expected, the energy decreases linearly in accordance with a lower strain in forming the (10,10) structure.

F. Other coalesced structures

We found that the SW coalescence is applicable to a broad variety of shell structures formed from graphite. For example, the cap of a tube may coalesce to the wall of another so that a *T*-shaped shell is formed without the addition or removal of atoms and material (Fig. 7). The scenario is similar to the cap-to-cap case. First, a four-member ring is formed through rebonding [Fig. 7(a)]; second, a preliminary neck [Fig. 7(b)] is formed when the larger (than a heptagon) polygons are removed; third, the neck widens until all pentagons are removed. The final structure [Fig. 7(c)] has six heptagons which are not removable but can change their positions to adjust the shape of the junction. This *T*-shaped junction may serve as a three-terminal device similar to the *Y*-shaped tubes,[35] potentially useful for nanoscale electronics.

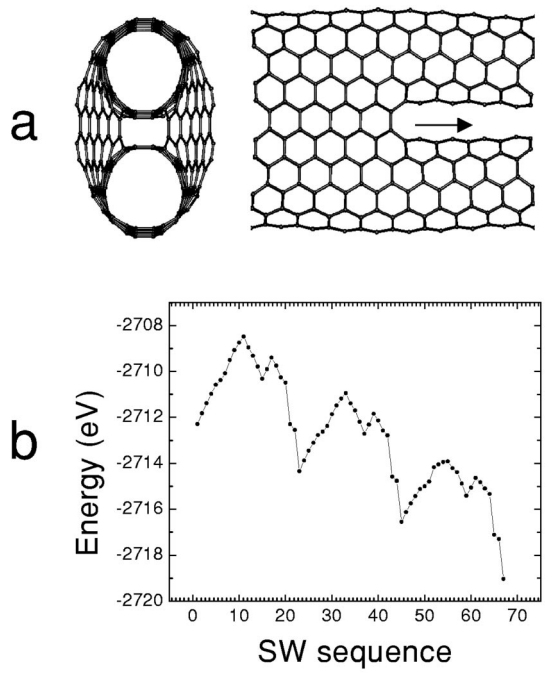

FIG. 6. Wall-to-wall coalescence of two parallel (5,5) tubes into a (10,10) tube. (a) Partly coalesced structure. The interface vault between the (10,10) tube and the (5,5) tubes is a 12-member ring (a hole). The propagation of the hole along the axis direction (arrow) will lead to complete coalescence. (b) Energy curve for three successive zipping cycles, each cycle consisting of 22 SW flips.

One more example illustrates the power of the proposed SW mechanisms. Through more than 200 SW rotations, a fullerene can penetrate through the perfect wall of a (10,10) tube, go inside, and separate in a stand-alone encapsulated C_{60} in a "peapod."[2,3] The intriguing but complicated process found and its physical plausibility are beyond the scope of this article.

IV. MOLECULAR DYNAMICS SIMULATION

We have performed MD simulations only for cap-to-cap coalescence of tubes. The high barrier for the cap fusion of larger tubes, (10,10) and (15,0), is difficult to overcome at a typical experimental temperature. However, similar to macroscopic sintering, the process can be facilitated by compression, as the energy is replaced by the enthalpy $E+fl$. The compression of (10 eV/Å) makes the energy path descend almost monotonously. A classical potential[22] chosen for MD simulations reproduces a roughly descending energy path corresponding to the predicted sequence. In this case, the process is only limited by the rate of individual SW flips.

In our MD simulation, if the temperature is set at $T = 3000$ K, the time needed for successful coalescence is $t \sim 1$ ns. One can estimate the average SW barrier as ~ 3.0 eV [from Eq. (1)], much lower than that in a perfect graphite

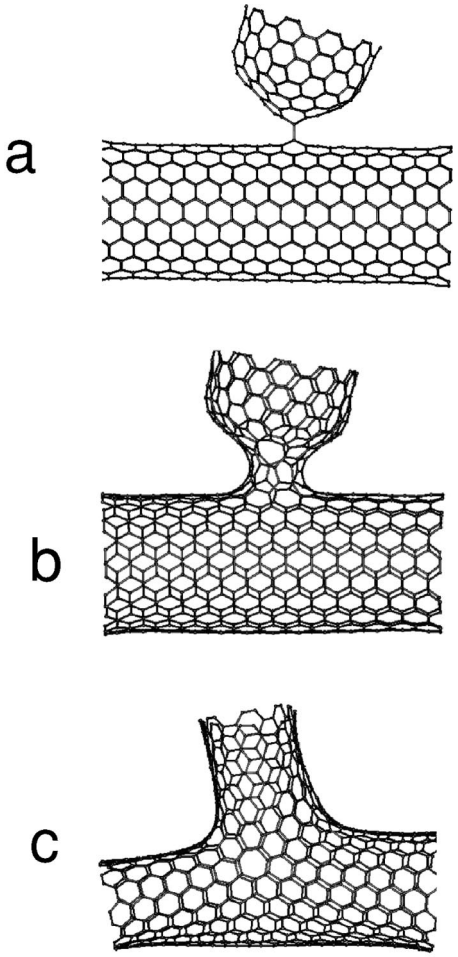

FIG. 7. Cap-to-wall coalescence: the cap of a (10,10) tube is first attached to the wall of another (10,10) tube through rebonding (a); 14 SW rotations heal the large holes and a neck is formed (b); 75 SW rotations lead to a T-shaped junction (c).

lattice.[30] Two reasons might account for this barrier reduction: first, all the bonds to be rotated are oriented roughly along the axis and therefore their rotation is enhanced by the external compression; second, the bonds are always in a defective environment (pentagons and/or heptagons) and the rotations lead to healing of the defects.

In actual simulations, the positions and forces were updated every 0.5 fs, so that a MD job runs about 2×10^6 steps. To compress the system, one open end was fixed while the other one was forced to move at a constant speed of G/t, where G is the initial gap between the caps.

Basically, the predicted neck growth is seen in all cases. We found that the fast coalescence of (5,5) tubes can be achieved at lower temperature (2500 K) while the larger ones can only be fused at 3000 K or higher. Fusion of (15,0) tubes is easier than that of (10,10) tubes. This is consistent with the energy paths. Several details of the simulation results corroborate our theoretical analysis. (a) Almost perfect (5,0), (5,5), and (10,0) necks can be seen. (b) In all cases after coalescence, there is very little mixing of the atoms belonging to the two original tubes. That is, there are very few exchanges of atoms between the two sides. (c) In cases

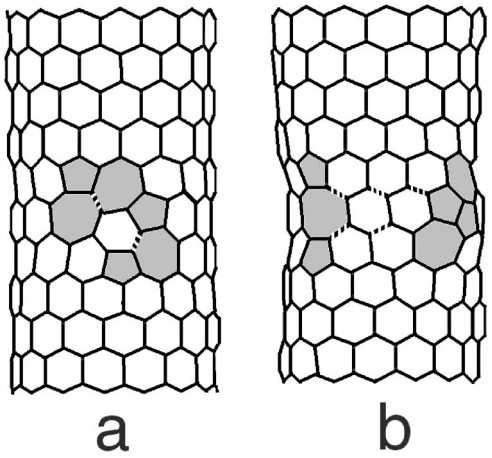

FIG. 8. Some defective final structures of coalesced (15,0) caps after MD simulations for 0.5 ns at 3000 K. (a) Normal defects. By SW rotations of the specified bonds, the defects can be removed and perfect tubes formed. (b) Ad-dimer and the dimmer vacancies. The SW rotations shown happened to relax the tube into the structure in (a).

where the simulation terminates before perfect tubes are formed, the defects in the tubes are SW reducible: i.e., they can be removed by SW rotations [see Fig. 8(a)].

Because of the very high temperature in MD simulations, some atoms protruded out of the shell at some stages, while vacancies were created elsewhere. But these defects can always be removed by relaxation. As a simple example, we show here an ad-dimer (7/5/5/7) and a dimer vacancy (5/8/5) in the (15,0) tube produced from a MD simulation. Mass transport from the ad-dimer to the dimer vacancy is accomplished by the SW rotations in Fig. 8(b). After the rotations, the defect evolves into the one in Fig. 8(a); then the same SW rotations will remove the defects, making the ad-dimer and dimer vacancy combine completely.

We found that the quality of coalescence can be improved by an alternating stress (compression tension) superimposed on the compression. This is because random defects like those shown in Fig. 8(b) are unavoidable and the SW flips to remove them are promoted by stretching in the axial direction. The local pileups of atoms resulting from compression can be smeared out more easily under temporary stretching.

V. DISCUSSION AND CONCLUSION

It is instructive to compare the cap-cap coalescence with its 3D counterpart, quantum point contact,[36] performed by a scanning tunneling microscope (STM). In the latter case, when a STM tip is approaching the sample, a so-called ''jump-to-contact'' event is first triggered, then followed by plastic deformation in the merging of the two parts. This general feature is preserved in the proposed coalescence sequence of CNT caps. The initial step—i.e., rebonding—is actually a ''jump-to-contact'' event, while the following SW rotations account for a plastic deformation process. In contrast to Ref. 36, this coalescence process is confined to a 2D shell structure and is therefore more transparent. Since a current or an electrical pulse, which is often applied in nanofab-

rication and atomic manipulation, is found to be able to accelerate or enhance mass transport in 3D nanojunctions,[37–39] it can be expected that the above cap-to-cap coalescence might be also triggered by an electric pulse applied to the cap-cap junction and accelerated by current through the formed neck.

In summary, we present atomically precise routes for complete coalescence of generic fullerene cages: C_{60} and CNT's merging cap-to-cap, cap-to-wall, and wall-to-wall to form a defect free final structure. The entire process is reduced to a sequence of SW bond switches and therefore is likely to represent the lowest energy path for the transition. The approach remains valid for arbitrary tubes with the important constraint of grain boundaries for tubes of different chirality. The junction of (n,m) and (n',m') must contain 5/7 dislocations or their equivalent of $(n-n',m-m')$ total Burgers vector.[17] The proposed mechanism has important implications for nanotube material (crystals, ropes) processing and property enhancement, engineering of nanoscale junctions of various types, and possible CNT growth mechanisms with the C_{60} and other nanoparticles as feedstock.

Finally, based on the present analysis, one can speculate that the fraction and coalescence of nanocrystals can be performed reversibly if little or none of the configuration entropy is produced in an adequately slow cycle. While a tensile force causes necking and separation into two properly capped fragments, upon compression, these fragments can possibly be brought together and healed seamlessly. A very recent experiment with CNT yarns[40] demonstrates an enhancement of strength and conductivity, attributed to a welding effect occurring at the connection points, a process very similar to what is described above and previously.[10]

ACKNOWLEDGMENTS

This work is supported by the AFOSR and Materials Directorate, Air Force Research Laboratory, and the Office of Naval Research, DURINT grant. Y.Z. thanks Donald Yeh and Clifford Yapp for assistance.

*Corresponding author. Electronic address: biy@rice.edu.

[1] S. Wang and P. R. Buseck, Chem. Phys. Lett. **182**, 1 (1991).
[2] B. W. Smith and D. E. Luzzi, Chem. Phys. Lett. **321**, 169 (2000).
[3] J. Sloan, R. E. Dunin-Borkowski, J. L. Hutchison, K. S. Coleman, V. C. Williams, J. B. Claridge, A. P. E. York, C. Xu, S. R. Bailey, G. Brown, S. Friedrichs, and M. L. H. Green, Chem. Phys. Lett. **316**, 191 (2000).
[4] S. Bandow, M. Takizawa, K. Hirahara, M. Yudasaka, and S. Iijima, Chem. Phys. Lett. **337**, 48 (2001).
[5] Y. Xia, Y. Xing, C. Tan, and L. Mei, Phys. Rev. B **53**, 13 871 (1996).
[6] M. Terrones, H. Terrones, F. Banhart, J.-C. Charlier, and P. M. Ajayan, Science **288**, 1226 (2000).
[7] P. Nikolaev, A. Thess, A. G. Rinzler, D. T. Colbert, and R. E. Smalley, Chem. Phys. Lett. **266**, 422 (1997); S. L. Fang, A. M. Rao, P. C. Eklund, P. Nikolaev, A. G. Rinzler, and R. E. Smalley, J. Mater. Res. **13**, 2405 (1998).
[8] D. B. Geohegan, H. Schittenhelm, X. Fan, S. J. Pennycook, A. A. Puretzky, M. A. Guillorn, D. A. Blom, and D. C. Joy, Appl. Phys. Lett. **78**, 3307 (2001); see also R. E. Smalley, Nav. Res. Rev. **18**, 3 (1991).
[9] R. R. Schlittler, J. W. Seo, J. K. Gimzewski, C. Durkan, M. S. M. Saifullah, and M. E. Welland, Science **292**, 1136 (2001). There are certain difficulties with reproducing this synthesis and at least in one case the product obtained under similar conditions reportedly has different chemical composition: A. R. Lupini *et al.* (unpublished).
[10] Y. Zhao, B. I. Yakobson, and R. E. Smalley, Phys. Rev. Lett. **88**, 185501 (2002).
[11] T. G. Schmalz, W. A. Seitz, D. J. Klein, and G. E. Hite, Chem. Phys. Lett. **130**, 203 (1986).
[12] M. Fujita, R. Saito, G. Dresselhaus, and M. S. Dresselhaus, Phys. Rev. B **45**, 13 834 (1992).
[13] D. J. Wales, M. A. Miller, and T. R. Walsh, Nature (London) **394**, 758 (1998); D. J. Wales and H. A. Scheraga, Science **285**, 1368 (1999).
[14] B. R. Eggen, M. I. Heggie, G. Jungnickel, C. D. Latham, R. Jones, and P. R. Briddon, Science **272**, 87 (1996).
[15] G. E. Scuseria, Science **271**, 942 (1996).
[16] A. J. Stone and D. J. Wales, Chem. Phys. Lett. **128**, 501 (1986).
[17] B. I. Yakobson, Appl. Phys. Lett. **72**, 918 (1998); M. B. Nardelli, B. I. Yakobson, and J. Bernholc, Phys. Rev. Lett. **81**, 4656 (1998); H. F. Bettinger, T. Dumitrica, G. E. Scuseria, and B. I. Yakobson, Phys. Rev. B **65**, 041406 (2002).
[18] M. S. Dresselhaus, G. Dresselhaus, and P. C. Eklund, *Science of Fullerenes and Carbon Nanotubes* (Academic Press, San Diego, 1996).
[19] The rigidity of a material depends on the mean coordination of the atoms in it. See D. J. Jacobs and M. F. Thorpe, Phys. Rev. Lett. **75**, 4051 (1995); Phys. Rev. E **53**, 3682 (1996).
[20] B. I. Yakobson, C. J. Brabec, and J. Bernholc, Phys. Rev. Lett. **76**, 2511 (1996).
[21] W. Humphrey, A. Dalke, and K. Schulten, J. Mol. Graphics **14**, 33 (1996).
[22] J. Tersoff, Phys. Rev. B **37**, 6991 (1988); D. W. Brenner, *ibid.* **42**, 9458 (1990).
[23] D. Porezag, T. Frauenheim, T. Kohler, G. Seifert, and R. Kaschner, Phys. Rev. B **51**, 12 947 (1995); see also C. M. Goringe, D. R. Bowler, and E. Hernandez, Rep. Prog. Phys. **60**, 1447 (1997). The TBA code implementation was kindly provided by Eduardo Hernandes, Institut de Cincia de Materials de Barcelona.
[24] M. J. Frisch *et al.*, computer code GAUSSIAN 98, revision A.6, Gaussian Inc., Pittsburgh, 1998.
[25] D. Porezag, M. Pederson, T. Frauenheim, and T. Kohler, Phys. Rev. B **52**, 14 963 (1995).
[26] *Fullerene Polymers and Fullerene Polymer Composites*, edited by P. C. Eklund and A. M. Rao (Springer, Berlin, 2000); A. M. Rao, P. Zhou, K. A. Wang, G. T. Hager, J. M. Holden, Y. Wang, W.-T. Lee, X.-X. Bi, P. C. Eklund, D. S. Cornett, M. A. Duncan, and I. J. Amster, Science **259**, 955 (1993).
[27] M. Terrones, H. Terrones, and W. K. Hsu, Chem. Soc. Rev. **24**, 341 (1995) and references therein.
[28] D. L. Strout, R. L. Murry, C. Xu, W. C. Eckhoff, G. K. Odom, and G. E. Scuseria, Chem. Phys. Lett. **214**, 576 (1993).

[29] V. H. Crespi, L. X. Benedict, M. L. Cohen, and S. G. Louie, Phys. Rev. B **53**, R13 303 (1996).
[30] Ge. Samsonidze, Gu. Samsonidze, and B. I. Yakobson, Phys. Rev. Lett. **88**, 065501 (2002).
[31] D. Orlikowski, M. B. Nardelli, J. Bernholc, and C. Roland, Phys. Rev. Lett. **83**, 4132 (1999).
[32] See the EPAPS material for Ref. 10, available via the entry for that article at http://prl.aps.org. Full proposed sequences corresponding to Figs. 3 and 5 are animated as MPG files, together with the MD simulation of the (10, 10) pair.
[33] B. I. Yakobson, Ge. Samsonidze, and Gu. Samsonidze, Carbon **38**, 1675 (2000).
[34] T. Kawai, Y. Miyamoto, O. Sugino, and Y. Koga, Phys. Rev. Lett. **89**, 085901 (2002).
[35] A. N. Andriotis, M. Menon, D. Srivastava, and L. Chernozatonskii, Phys. Rev. Lett. **87**, 066802 (2001).
[36] U. Landman, W. D. Luedtke, B. E. Salisbury, and R. L. Whetten, Phys. Rev. Lett. **77**, 1362 (1996); U. Landman, W. D. Luedtke, N. A. Bernham, and R. J. Colton, Science **248**, 454 (1990).
[37] Q. J. Gu, N. Liu, W. B. Zhao, Z. L. Ma, Z. Q. Xue, and S. J. Pang, Appl. Phys. Lett. **66**, 1747 (1995).
[38] R. S. Becker, J. A. Golovchenko, and S. Swartzentruber, Nature (London) **325**, 419 (1987).
[39] D. M. Eigler and E. K. Schweizer, Nature (London) **344**, 524 (1990).
[40] K. Jiang, Q. Li, and S. Fan, Nature (London) **419**, 801 (2002).